Effect of Mg^{2+} on Solution Conformation of Two Different Transfer Ribonucleic Acids†

John C. Thomas,* J. Michael Schurr, Brian R. Reid, N. Susan Ribeiro, and Dennis R. Hare

ABSTRACT: We have investigated the effect of Mg^{2+} on the solution conformation of two different tRNAs by studying the decay of the fluorescence polarization anisotropy of intercalated ethidium on a nanosecond time scale. In the presence of endogenous Mg^{2+}, yeast $tRNA^{Phe}$ and *Escherichia coli* $tRNA_1^{Val}$ exhibit similar behavior; i.e., the fluorescence from the intercalated ethidium decays biexponentially with lifetimes of ~25 and ~5 ns, and the fluorescence polarization anisotropy decays with a lifetime of ~25 ns. However, once Mg^{2+} is removed from the two tRNAs, their behavior is no longer similar. In the case of yeast $tRNA^{Phe}$, it appears that titrating with Mg^{2+} restores the tRNA to the condition that it was in prior to the Mg^{2+} removal. This is not so for *E. coli* $tRNA_1^{Val}$, in which case titrating with Mg^{2+} results in a two-component anisotropy decay with lifetimes of ~25 and ~6 ns. Rudimentary calculations indicate that the 6-ns component does not result simply from a change in conformation of the tRNA. However, torsional motions in the tRNA facilitated by a torsion "joint" with a rigidity $\sim^1/_{40}$ that of intact linear ϕ29 DNA would yield a decay component on this time scale with about the right amplitude. We are thus left with the possibility that (after initially removing magnesium) titrating $tRNA_1^{Val}$ with Mg^{2+} leads to increased internal flexibility and a significant amplitude of a deformational relaxation mode. At any rate, there is no question that after removal of Mg^{2+} $tRNA^{Phe}$ and $tRNA_1^{Val}$ display quite different solution conformation behavior. These findings are in qualitative aggreement with recent 500-MHz ^1H NMR results from solutions of these two tRNAs.

Over the past several years, considerable evidence has become available to support the notion that tRNAs may exist in a number of different conformations in solution (one of which may be the crystal structure) and, further, that this conformational variability may be essential for recognition by proteins during translation [see review by Rigler & Wintermeyer (1983) and Favre & Thomas (1981)].

In a series of fluorescence lifetime and nanosecond depolarization measurements on ethidium bromide (EB) intercalated into unfractionated yeast tRNA and purified yeast $tRNA^{Phe}$, Tao et al. (1970) found that the overall conformation of crude tRNA was significantly affected by magnesium ions whereas yeast $tRNA^{Phe}$ was less affected. Subsequently, Ehrenberg et al. (1979) performed a similar set of experiments on yeast $tRNA^{Phe}$ with EB covalently attached (rather than intercalated) into the D loop and the anticodon loop. Ehrenberg et al. interpreted their data in terms of three conformational states for $tRNA^{Phe}$, the equilibrium beween the states being a function of both Mg^{2+} and temperature. At high Mg^{2+} to $tRNA^{Phe}$ ratios, the predominant conformation was identified with the crystal structure.

The observation of split methyl resonances in the NMR spectrum of *Escherichia coli* $tRNA_1^{Val}$ led Reid (1977) to deduce the existence of at least two conformations for this tRNA solution. Under the conditions used, the population of these two conformers was approximately 70:30, and their line widths indicated that exchange between the two states was relatively slow. On the basis of the molecular dimensions of aminoacyl-tRNA synthetase enzymes, Reid suggested a physically plausible model for synthetase–tRNA recognition consistent with much of the biochemical, biophysical, and crystallographic data. This model proposed that tRNA exists in solution as an equilibrium between "L-shaped" and "U-shaped" conformers and that it is the U conformer with its anticodon folded up onto its acceptor end that interacts with the synthetase. This possibility is particularly appealing in light of the molecular dynamics calculations of Harvey & McCammon (1981), which show that for $tRNA^{Phe}$ the energy barrier between an L shape (i.e., the crystal structure) and a more compact U (or V?) shape is only ~50 kcal/mol. The actual energy difference between these two states is only ~10 kcal/mol or the equivalent of a couple of hydrogen-bond energies.

More recently, Nilsson et al. (1982) have interpreted their small-angle X-ray scattering data from the $tRNA^{Phe}$–$tRNA_2^{Glu}$ dimer complex in terms of a model in which the two tRNAs, bound via their anticodons, adopt a conformation wherein the acceptor arms are folded toward the anticodon arms rather than being at right angles as they are in the crystal structure. These authors infer from their data that codon–anticodon interaction favors a tRNA conformation more compact than the crystal structure and that conformational changes of the whole tRNA molecule involving relative movement of the two tRNA arms may be important in many tRNA interactions.

If one accepts that tRNAs may have a range of conformations in solution and that particular conformations may prevail under certain solution conditions, it is appropriate to ask whether, under the same solution conditions, *different* tRNAs might adopt different conformations. Recent 500-MHz ^1H NMR studies (D. Hare and B. R. Reid, unpublished results; Hare, 1983) of yeast $tRNA^{Phe}$ and *E. coli* $tRNA_1^{Val}$ as a function of temperature and magnesium ion indicate possible differences in tertiary structure between these two tRNAs. Specifically, the NMR spectra for both tRNAs show similar features, but the $tRNA_1^{Val}$ spectra invariably have narrower lines than do the $tRNA^{Phe}$ spectra. This is particularly apparent at low Mg^{2+} concentrations. For $tRNA_1^{Val}$, we also observed unexpected lability in the secondary base pairs at the base of the acceptor helix and the top of the anticodon. Also, for $tRNA_1^{Val}$ a Mg^{2+}-dependent chemical shift in the 15–48 tertiary base pair was observed.

To investigate further the possibility of structural differences between yeast $tRNA^{Phe}$ and *E. coli* $tRNA_1^{Val}$, we have carried out a series of nanosecond fluorescence polarization anisotropy

† From the Department of Chemistry, University of Washington, Seattle, Washington 98195. *Received January 4, 1984.* This work was supported in part by NSF Grant PCM 228022.

0006-2960/84/0423-5414$01.50/0 © 1984 American Chemical Society

(FPA) experiments on EB complexes of the two tRNAs. The results of this work are presented below.

Materials and Methods

tRNA Samples. Yeast $tRNA^{Phe}$ was purchased from Boehringer-Mannheim and used without further purification. Pure *E. coli* $tRNA_1^{Val}$ was prepared as previously described (Reid et al., 1977; Thomas et al., 1984). When Mg^{2+} was removed from the tRNA samples, this was done by dissolving 10–16 mg of tRNA in 10 mL of 10 mM EDTA (ethylenediaminotetraacetic acid) at pH 7.0 and heating the solution to 80 °C for 5 min. The solution was allowed to cool slowly to 25 °C followed by vacuum dialysis against 10 mM phosphate buffer at pH 7.0 down to a final solution volume of 0.4 mL at 25 °C. After this treatment, the $tRNA_1^{Val}$ was assayed by aminoacylation with ^{14}C-labeled valine by using partially purified valyl-tRNA synthetase. The acceptor activity was 1100 pmol/A_{260} unit, corresponding to a functional activity of 60% of the pure untreated $tRNA_1^{Val}$. Polyacrylamide gel electrophoresis indicated no nicking or internal cleavage of the $tRNA_1^{Val}$ by this treatment. The treated $tRNA_1^{Val}$ (1.3 A_{260} units) was first heated to 60 °C for 1 min in a denaturing buffer (0.09 M Tris [tris(hydroxymethyl)aminomethane] + 0.09 M sodium borate, 1 mM EDTA, 8 M urea, 0.025% xylene cyanols, 0.025% bromophenol blue). It was then electrophoresed on a denaturing 12% polyacrylamide gel. The gel was stained with acridine orange and destained and the tRNA visualized under UV light (260 nm). Even when large amounts of tRNA were applied, all of the material migrated as intact tRNA with virtually no faster migrating bands corresponding to smaller oligonucleotides produced by tRNA cleavage.

For the FPA experiments, samples were diluted to a concentration of 0.5 mg/mL with 10 mM phosphate buffer and adjusted to 0.1 M in NaCl. Ethidium bromide was added in the proportion of 1 EB per 20 tRNA molecules. The Mg^{2+} concentration was increased by adding aliquots of concentrated $MgCl_2$. The FPA experiments were also carried out on tRNA samples that were not subjected to the EDTA heat treatment; these latter samples were independently estimated to contain 2–4 mol of residual bound Mg^{2+}/mol of tRNA.

FPA Measurements. These measurements were carried out with a picosecond pulsed dye laser as the excitation source and time-correlated single-photon counting to detect the resultant ethidium fluorescence emission. The dye laser output consisted of 15-ps fwhm pulses at 575 nm, and the fluorescence emission beyond 630 nm was detected. A combination of polarizer, polarization rotator, and analyzer allowed selection of the fluorescence components with polarization parallel and perpendicular to the initial laser polarization. This system has been described previously in considerable detail (Thomas et al., 1980; Thomas & Schurr, 1983).

The sample was contained in a quartz cuvette, which in turn was enclosed in a jacketted housing. The temperature of the sample was maintained at 20.0 ± 0.1 °C by a VWR Model 90T water bath.

Data Analysis. The experimental decay curves obtained are the sum or total fluorescence $s(t)$ and the difference between the two fluorescence polarization components $d(t)$. These measured data are actually convolutions of the instrument response function $e(t)$ and the true decay curves $S(t)$ and $D(t)$, respectively. A locally written nonlinear least-squares fitting routine using a convolute-and-compare method was used to determine the best fit curves for $S(t)$ and $r(t) = S(t)/D(t)$. Here, $r(t)$ is the time-dependent fluorescence polarization anisotropy, which describes the Brownian rotational motion of the $tRNA_1^{Val}$/ethidium complex. $S(t)$ was modeled by a single exponential decay (or a sum of exponentials).

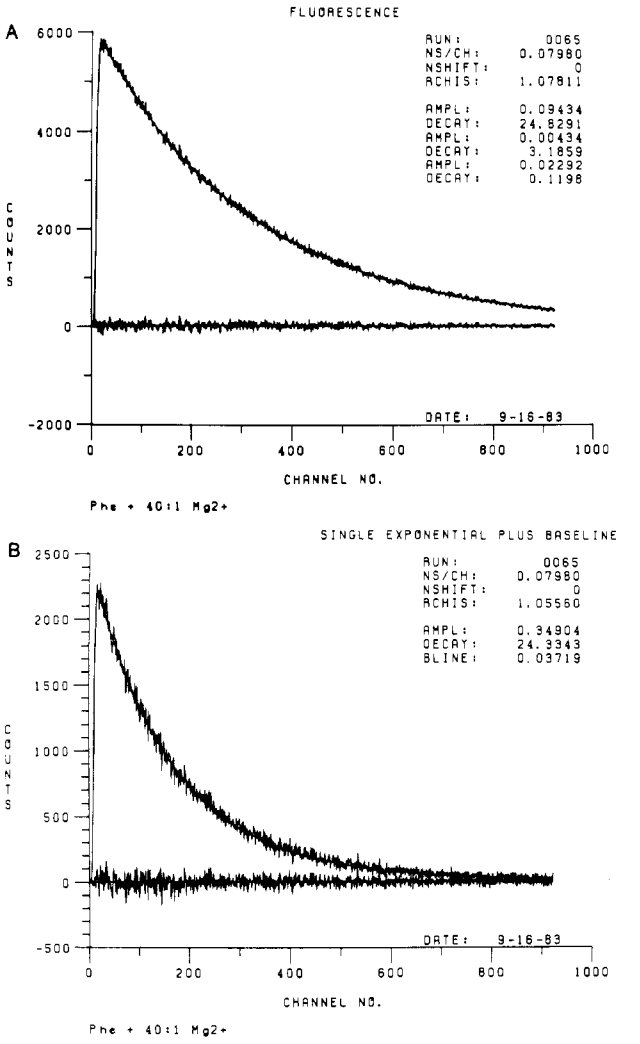

FIGURE 1: (A) Experimental sum fluorescence response $s(t)$ for EB/$tRNA^{Phe}$ on a timescale of 0.0798 ns/channel. The data are fitted to three exponentials [convoluted with the instrument response $e(t)$]: $tRNA^{Phe}$ concentration 0.5 mg/mL, 5% EB coverage, and 40:1 mole ratio Mg^{2+}. (B) Experimental difference data $d(t)$ for $tRNA^{Phe}$ and the best fit curve with a single exponential plus base line for $r(t)$: timescale 0.0798 ns/channel, $tRNA^{Phe}$ concentration 0.5 mg/mL, 5% EB coverage, and 40:1 mole ratio Mg^{2+}.

Assuming that tRNA can be reasonably described as a prolate ellipsoid of revolution with a suitable axial ratio, we have routinely attempted to fit $r(t)$ to a sum of exponentials plus a base line that could be fixed (e.g., at 0.0) or determined in the fitting process. All data analyses were carried out on a VAX 11/780 computer.

Results

In all cases, the total fluorescence from either tRNA decayed in an essentially biexponential fashion, although occasionally (and intermittently) a third component with a lifetime $\lesssim$200 ps had to be introduced to fit the data well. We have previously noted (Thomas & Schurr, 1983) that this short-time component, which can be removed by shifting the raw data in time (by 1–2 channels), is almost certainly due to small timing fluctuations in our detection system and is not due to emission from this samples. Figures 1 and 2 show representative experimental data sets along with their best-fit curves on a time scale of 0.0798 ns/channel. Figure 1A is a plot of the sum data (fluorescence) $s(t)$ for $tRNA^{Phe}$ in the presence

Table I: Fluorescence and Anisotropy Parameters for $tRNA^{Phe}$

Mg^{2+} per tRNA	fluorescence[a]				anisotropy[b]		
	a_1	τ_1 (ns)	a_2	τ_2 (ns)	r_0	τ_R (ns)	r_∞
0	0.931 ± 0.01	25.06 ± 0.06	0.069 ± 0.01	2.58 ± 0.9	0.339 ± 0.003	21.35 ± 0.3	0.058 ± 0.01
1	0.951 ± 0.007	25.06 ± 0.05	0.049 ± 0.007	4.22 ± 0.9	0.339 ± 0.002	21.22 ± 0.8	0.057 ± 0.01
5	0.937 ± 0.01	24.95 ± 0.3	0.063 ± 0.01	4.26 ± 2	0.342 ± 0.002	22.52 ± 0.7	0.058 ± 0.03
10	0.951 ± 0.01	24.80 ± 0.08	0.049 ± 0.01	4.03 ± 1.5	0.347 ± 0.004	23.73 ± 0.4	0.049 ± 0.006
20	0.956 ± 0.004	24.84 ± 0.05	0.044 ± 0.004	3.46 ± 0.6	0.347 ± 0.002	23.91 ± 0.8	0.046 ± 0.02
40	0.944 ± 0.02	24.76 ± 0.08	0.056 ± 0.02	2.96 ± 1.0	0.350 ± 0.003	24.54 ± 0.6	0.041 ± 0.006
40[c]	0.958 ± 0.02	24.33 ± 0.08	0.042 ± 0.02	1.77 ± 0.2	0.359 ± 0.01	25.97 ± 0.5	0.026 ± 0.01
40[d]	0.946 ± 0.01	24.70 ± 0.2	0.054 ± 0.01	4.21 ± 1.7	0.347 ± 0.01	24.02 ± 0.9	0.051 ± 0.01
int[e]	0.892 ± 0.01	24.36 ± 0.3	0.108 ± 0.01	4.59 ± 2	0.320 ± 0.04	25.90 ± 1.3	0.098 ± 0.01

[a] $S(T) = a_1 \exp(-t/\tau_1) + a_2 \exp(-t/\tau_2)$. $a_1 + a_2 = 1.0$. [b] $r(t) = r_0 \exp(-t/\tau_R) + r_\infty$. [c] Solution left 4 days at 4 °C. [d] Solution heated to 65 °C for 10 min and allowed to cool slowly to 20 °C. [e] $tRNA^{Phe}$ with endogenous Mg^{2+}.

Table II: Fluorescence and Anisotropy Parameters for $tRNA_1^{Val}$

Mg^{2+} per tRNA	fluorescence[a]				anisotropy[b]		
	a_1	τ_1 (ns)	a_2	τ_2 (ns)	r_0	τ_R (ns)	r_∞
0	0.888 ± 0.003	24.30 ± 0.03	0.112 ± 0.003	6.84 ± 0.9	0.314 ± 0.002	20.14 ± 0.3	0.062 ± 0.001
1	0.881 ± 0.01	24.21 ± 0.2	0.119 ± 0.01	7.48 ± 0.7	0.310 ± 0.002	18.19 ± 0.4	0.070 ± 0.007
5	0.870 ± 0.003	24.11 ± 0.1	0.130 ± 0.003	7.48 ± 0.7	0.310 ± 0.003	17.63 ± 0.4	0.077 ± 0.003
10	0.873 ± 0.01	23.92 ± 0.2	0.127 ± 0.01	7.39 ± 0.8	0.311 ± 0.001	17.01 ± 0.6	0.075 ± 0.004
20	0.870 ± 0.009	23.94 ± 0.1	0.130 ± 0.009	8.38 ± 0.3	0.311 ± 0.002	16.62 ± 0.3	0.068 ± 0.006
40	0.863 ± 0.02	23.82 ± 0.2	0.137 ± 0.02	8.51 ± 0.9	0.310 ± 0.003	16.21 ± 0.2	0.062 ± 0.01
40[c]	0.904 ± 0.004	23.57 ± 0.2	0.096 ± 0.004	6.30 ± 0.09	0.317 ± 0.001	17.23 ± 0.3	0.057 ± 0.01
40[d]	0.836 ± 0.004	21.82 ± 0.3	0.164 ± 0.03	7.93 ± 1.0	0.304 ± 0.02	11.04 ± 0.1	0.065 ± 0.007
int[e]	0.914 ± 0.01	25.65 ± 0.2	0.086 ± 0.01	5.61 ± 0.9	0.341 ± 0.004	24.41 ± 1.8	0.057 ± 0.009

[a] $S(T) = a_1 \exp(-t/\tau_1) + a_2 \exp(-t/\tau_2)$. $a_1 + a_2 = 1.0$. [b] $r(t) = r_0 \exp(-t/\tau_R) + r_\infty$. [c] Solution left 4 days at 4 °C. [d] Solution heated to 65 °C for 10 min and allowed to cool slowly to 20 °C. [e] $tRNA_1^{Val}$ with endogenous Mg^{2+}.

of a 40:1 mole ratio of Mg^{2+}. Also shown in the figure is a plot of the residuals between the experimental data and the fitted curve. In this case, the data were fitted to three exponential decay components [convoluted with the instrument response $e(t)$]. It is evident from the figure that the best fit curve fits the data exceedingly well and that the residuals are evenly distributed about zero with no systematic variation. Furthermore, the reduced χ^2 is close to the value $x_r^2 = 1.0$, which is expected when the particular functional form is a good representation of the data and when the standard deviation of the data is independently known (Bevington, 1969).

Figure 1B shows the corresponding difference data $d(t)$ and the best fit curve, which in this case is found by modeling $r(t)$ with a single exponential plus a free base line. Again, we see that the data are well fitted by the functional form chosen. Figure 2A,B shows similar data for $tRNA_1^{Val}$.

Tables I and II show the variation of the best fit parameter values for the fluorescence and the anisotropy as a function of added Mg^{2+} over the range 0–40 Mg^{2+}/tRNA for both tRNAs. The data values listed in the tables are obtained by averaging five sets of data like those shown in Figures 1 and 2. The uncertainty is the standard deviation of the five data sets. Here, τ_1 and τ_2 are the fluorescence lifetimes, and we have ignored the intermittent 100–200-ps component as an instrumental artifact. τ_R is the anisotropy relaxation time, and we identify this with the rotational relaxation time of the EB/tRNA complex.

Examination of the data in Table I reveals that for yeast $tRNA^{Phe}$ the fluorescence has two components at all magnesium concentrations studied. The majority component has a lifetime τ_1 close to 25 ns and accounts for ~93–96% of the signal. The remaining 4–7% of the decay is due to a component with a lifetime $\tau_2 \sim 3$–4 ns. There is also the suggestion that both lifetimes decrease somewhat with increasing Mg^{2+} concentration. We have previously suggested (Thomas et al., 1984) that these two components may be associated with a larger population that contains intercalated ethidium (the major, 25-ns component) and a much smaller population with ethidium bound to a more open part of the tRNA molecule, perhaps in the P_{10} cavity, giving rise to the short-lifetime component.

Turning to the anisotropy parameters, we see that for yeast $tRNA^{Phe}$ both the anisotropy amplitude r_0 and the decay time τ_R increase steadily with increasing Mg^{2+} concentration. At 40 Mg^{2+}/tRNA, $\tau_R = 24.5$ ns, which is close to the value of 25.9 ns that we found for the yeast $tRNA^{Phe}$ sample that was not heated in EDTA to remove Mg^{2+} (see last row in Table I). Furthermore, leaving the tRNA in the presence of 40:1 Mg^{2+} for 4 days or heating the tRNA to 65 °C and allowing it to reanneal do not cause any further change in the anisotropy behavior. Thus, it seems that at 40:1 Mg^{2+} the EDTA-heated $tRNA^{Phe}$ has returned to its "normal" state. These results are in essential agreement with the idea that addition of Mg^{2+} leads to a more extended, rigid tRNA conformer with larger rotational relaxation times (Rigler & Wintermeyer, 1983; Ehrenberg et al., 1979).

The data in Table II show that the fluorescence emission from EB/$tRNA_1^{Val}$ is very similar to that from EB/$tRNA^{Phe}$; i.e., it shows a biphasic decay that is dominated by the long-lived component. These are however a number of subtle differences between the $tRNA_1^{Val}$ data and the data for $tRNA^{Phe}$. In the $tRNA_1^{Val}$ case, although the long-lived component still dominates the decay, it accounts for only ~86–89% of the total signal, instead of 93–96%. Furthermore, the lifetime of this component is about 1 ns shorter than the corresponding long lifetime in $tRNA^{Phe}$, and the short-lived component is almost twice as long as that in $tRNA^{Phe}$. In the course of these experiments it was observed that, under identical conditions of tRNA and EB concentration, the fluorescence emission from EB/$tRNA_1^{Val}$ was almost exactly twice as strong as that from EB/$tRNA^{Phe}$. Evidently, there are subtle but significant differences in the manner and/or

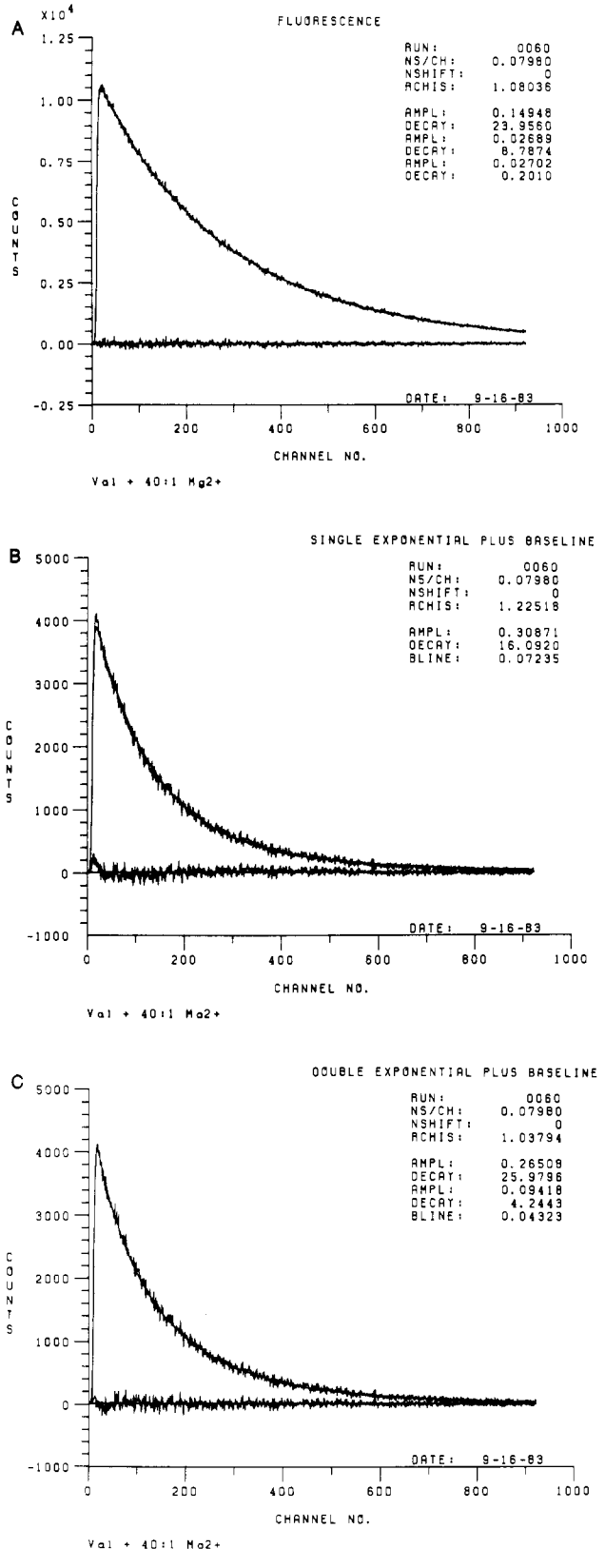

FIGURE 2: (A) Experimental sum fluorescence response $s(t)$ for EB/tRNA$_1^{Val}$ on a timescale of 0.0798 ns/channel. The data are fitted to three exponentials [convoluted with the instrument response $e(t)$]: tRNA$_1^{Val}$ concentration 0.5 mg/mL, 5% EB coverage, and 40:1 mole ratio Mg^{2+}. (B) Experimental difference data $d(t)$ for tRNA$_1^{Val}$ and the best fit curve with a single exponential plus base line for $r(t)$: timescale 0.0798 ns/channel, tRNA$_1^{Val}$ concentration 0.5 mg/mL, 5% EB coverage, and 40:1 mole ratio Mg^{2+}. (C) Experimental difference data $d(t)$ for tRNA$_1^{Val}$ and the best fit curve with a double exponential plus base line for $r(t)$: timescale 0.0798 ns/channel, tRNA$_1^{Val}$ concentration 0.5 mg/mL, 5% EB coverage, and 40:1 mole ratio Mg^{2+}.

site of EB binding to these two tRNAs.

The most significant difference between tRNA$_1^{Val}$ and tRNA^{Phe} occurs in the behavior of the FPA decay. Table II shows that, in contrast to EB/tRNA^{Phe}, as the Mg^{2+} concentration is increased the τ_R for EB/tRNA$_1^{Val}$ *decreases* quite significantly. Leaving the tRNA$_1^{Val}$ in 40:1 Mg^{2+} for a further 4 days has little effect, but heating the sample to 65 °C and allowing it to reanneal causes a substantial change in the tRNA. The dominant fluorescence lifetime decreases to $\tau_1 \sim 22$ ns, and τ_R decreases markedly to $\sim$11 ns. The fluorescence and anisotropy parameters obtained for tRNA$_1^{Val}$ in the presence of added Mg^{2+} and especially after heating in the presence of Mg^{2+} differ markedly from those shown in the last row of Table II, which are for tRNA$_1^{Val}$ from which the low level of endogenous Mg^{2+} has not been removed. Evidently, it is not possible to simply titrate in Mg^{2+} and restore the tRNA$_1^{Val}$ to the state it was in prior to the removal of Mg^{2+}. This is in contrast to the behavior of tRNA^{Phe}.

As the Mg^{2+} mole ratio increases, it becomes increasingly obvious that a single exponential plus base line model for $r(t)$ does not fit the difference data very well. At Mg^{2+} mole ratios $\gtrsim$5:1, the data can best be fitted to a double exponential plus base line. In Figure 2C we show the difference data $d(t)$ for tRNA$_1^{Val}$ with 40:1 Mg^{2+} fitted by using a double exponential plus base line model for $r(t)$. Comparing this plot with that of Figure 2B, which shows the same data fitted by assuming $r(t)$ to be a single exponential plus base line, we see that with two decay times the data are fitted much better at short times. Table III, which summarizes the results obtained from a two-component analysis, shows that the data contain one component with a decay time $\tau_R' \sim$ 28–30 ns, which accounts for $\sim$70% of the decay, and another component with a decay time $\tau_R'' \sim$ 5–6 ns contributing the remaining 30%. The decay times remain relatively constant as the Mg^{2+} concentration is increased, but the relative amplitude of the short-time component increases slightly. When the tRNA$_1^{Val}$ is heated to 65 °C and cooled, the two decay times are essentially unchanged, but the relative amplitude of the short-time component increases markedly, and it becomes the dominant decay component.

Discussion

Our finding with EB/tRNA^{Phe} that adding Mg^{2+} leads initially to longer rotational relaxation times that closely approach those measured for tRNA^{Phe} from which endogenous Mg^{2+} was not removed is in accord with previous views that Mg^{2+} is essential to maintain tRNA^{Phe} in its native conformation (Rigler & Wintermeyer, 1983). Our observation of two fluorescence decay components even without Mg^{2+} differs from the results of Tao et al. (1970), who detected only one decay component in the absence of Mg^{2+}. We have previously noted (Thomas et al., 1984) that, since the latter authors had lower time resolution than the present experiments and did not deconvolute their raw data, it would have been difficult to detect a small-amplitude ($\sim$7%), fast decay time ($\sim$3-ns) component. Thus, there is general agreement between the present and previous work on tRNA^{Phe}.

The behavior exhibited here by EB/tRNA$_1^{Val}$ is more intriguing. This, and other work (Thomas et al., 1984), indicates that, prior to the removal of magnesium, tRNA$_1^{Val}$ behaves quite similarly to tRNA^{Phe} and, in particular, these two tRNAs have essentially identical rotational relaxation times ($\sim$24–26 ns in water at 20 °C). However, once magnesium is removed, the behavior of *E. coli* tRNA$_1^{Val}$, as monitored by the fluorescence anisotropy decay, differs greatly from that of tRNA^{Phe}. Fitting the anisotropy data for tRNA$_1^{Val}$ with a

Table III: $tRNA_1^{Val}$ Anisotropy Fitted with Two Decay Components[a]

Mg^{2+} per tRNA	r_0'	τ_R (ns)	r_0''	τ_R'' (ns)	r_∞
5	0.262 ± 0.03	30.94 ± 9.7	0.099 ± 0.03	5.42 ± 3.0	0.045 ± 0.02
10	0.264 ± 0.03	27.81 ± 5.4	0.093 ± 0.03	5.11 ± 2.1	0.045 ± 0.02
20	0.255 ± 0.01	29.01 ± 3.8	0.105 ± 0.01	5.55 ± 1.2	0.035 ± 0.03
40	0.242 ± 0.02	30.27 ± 5.8	0.117 ± 0.03	6.18 ± 1.7	0.033 ± 0.03
40[b]	0.167 ± 0.009	24.83 ± 1.0	0.180 ± 0.02	6.15 ± 0.3	0.040 ± 0.007

[a] $r(t) = r_0' \exp(-t/\tau_R') + r_0'' \exp(-t/\tau_R'') + r_\infty$. [b] Solution heated to 65 °C and allowed to cool slowly to 20 °C.

single exponential gives a relaxation time that decreases upon addition of Mg^{2+}.

The simplest explanation of this behavior is that Mg^{2+} either physically compacts the tRNA or makes it more flexible so that its conformationally averaged hydrodynamic size is smaller. However, the fact that the anisotropy data can be resolved into two components at increasing Mg^{2+} concentration suggests that the situation is not that straightforward. Despite the pitfalls of extracting reliable parameter values from multiexponential data analyses, the second component is real and reproducible, and a more considered explanation must be offered. An extra anisotropy decay component would be expected if (i) a rearrangement occurred within the tRNA that changed the axial ratio and/or the angle between the EB emission dipole and the symmetry axis of the tRNA, (ii) the tRNA had two solution conformations, or (iii) there was increased internal flexibility (due perhaps to a "hinge") in the tRNA. We now consider each of these possibilities.

In the case of an ellipsoid of revolution, the parameter $r(t)$ will consist of up to three exponential components with relative amplitudes that depend on both the axial ratio of the ellipsoid and the angle between the transition dipole of the fluorescent probe and the symmetry axis (Tao, 1969). These results of Tao (1969) are correct when both absorption and emission take place along the same transition dipole, as is the case here, but not in more general situations, as shown by Ehrenberg & Rigler (1972), Belford et al. (1972), and Chuang & Eisenthal (1972). Tao et al. (1970) have pointed out that detection of a single anisotropy decay component means either that the tRNA may be taken to be spherical in shape or, more realistically, that if the tRNA is considered as a prolate ellipsoid of revolution, then the ethidium bromide emission dipole must be oriented at an angle θ near 0 or near 40° to the ellipsoid symmetry axis. Observation of two relaxation times in the anisotropy eliminates the possibility of a spherical geometry.

After heating the $tRNA_1^{Val}$ in the presence of Mg^{2+}, the anisotropy can be resolved into two components of comparable amplitudes with decay times of 24.8 and 6.2 ns (Table III). From an examination of the θ-dependence of the relative amplitudes of the anisotropy decay components [Figure 9 of Tao et al. (1970)], it is clear that the anisotropy decay will contain two components of comparable amplitude whenever $\theta \sim 27°$ or $\theta \sim 65°$. When $\theta \sim 27°$, the decay will be dominated by the lifetimes $\tau_1 = 1/(6D_\perp)$ and $\tau_2 = 1/(5D_\perp + D_\parallel)$. When $\theta \sim 65°$, the dominant lifetimes are τ_2 and $\tau_3 = 1/(2D_\perp + 4D_\parallel)$. Here, $D_\perp$ and $D_\parallel$ are the rotational diffusion coefficients for motion perpendicular and parallel to the (prolate) ellipsoid symmetry axis, respectively. The problem now is to decide whether we are seeing the combination τ_1 and τ_2 or τ_2 and τ_3. This question can be answered by examining the relationship between the ellipsoid axial ratio and the rotational relaxation times τ_1, τ_2, and τ_3. We observe relaxation times that differ from each other by a factor of 4. From Table III of Tao et al. (1970), we see that $\tau_1/\tau_2 \sim 4$ requires an axial ratio $\rho \sim 10$ and that $\tau_2/\tau_3 \sim 4$ implies $\rho > 20$. We need now to consider whether any possible conformation of $tRNA_1^{Val}$ could accomodate such large axial ratios.

The largest axial ratio that can be obtained for a tRNA that still has intact double helical regions occurs when the tRNA adopts a linear rodlike shape. In this case, the length would be ~12 nm and the diameter would be ~2.5 nm (the diameter of a nucleic acid; Yamakawa & Fujii, 1973). Thus, the axial ratio would be $\rho = 12/2.5 \sim 5$, which is much smaller than the values for ρ discussed above. We conclude that a simple change in axial ratio and/or EB binding angle could not give rise to the observed anisotropy parameters and therefore rule out possibility i above.

One of the anisotropy components has a relaxation time of 24.8 ns, which is essentially identical with the value $\tau_R = 24.4$ ns that we measure for "normal" $tRNA_1^{Val}$ (see last row of Table II), so it is tempting to assign this relaxation time to the presence of "normal" $tRNA_1^{Val}$ molecules in solution. The 6.2-ns component that we observe must then be due to a more compact $tRNA_1^{Val}$ species, i.e., perhaps a U-shaped conformer. We envisage the tRNA adopting a U shape by simply folding the tRNA in half with the anticodon loop positioned near the 3'-CCA end (Reid, 1977). Such a conformation requires relatively little rearrangement in the variable loop consisting of residues 44–48 (B. R. Reid, unpublished results). This would give the tRNA dimensions on the order of 5.1 nm long and 5.0 nm wide (i.e., two double helices in width). Using the formalism of Tao (1969), we calculate that a molecule of this size would have relaxation times $\tau_1 \sim 16.6$ ns, $\tau_2 \sim 16.6$ ns, and $\tau_3 \sim 16.5$ ns. These times are all considerably longer than the observed 6.2 ns, so we conclude that a simple folding of the $tRNA_1^{Val}$ molecule has not occurred. Evidently, a substantially more compact molecule is necessary to give rise to such a short anisotropy relaxation time.

Presumably, the smallest volume that the tRNA can occupy is when the molecule is in a fully compacted anhydrous state. This volume is difficult to calculate because an acceptable value for the physically occupied or hydrodynamic volume is not available. At one extreme is the value $v \sim 0.503$ mL/g used by Tao et al. (1970) for the partial specific volume. This value undoubtedly contains a contribution from electrostriction of the surrounding water and underestimates the hydrodynamic volume. At the other extreme is the value that we can calculate from dimensions of the double helix estimated from hydrodynamic measurements on DNA. Assuming a rise per base pair of 0.34 nm and a diameter of 2.5 nm (Yamakawa & Fujii, 1973), we calculate the hydrodynamic volume of a base pair as $v_{bp} \sim 1.52$ mL/g. These two values differ by a factor of 3, and it seems more reasonable to choose a value somewhere between the two. We prefer to use $v \sim 0.75$ mL/g, which is a typical value for proteins. Assuming a relative molar mass $M_r \sim 26000$ g/mol, we calculate the anhydrous volume of the tRNA to be $V_a \sim 32$ nm^3. A sphere of this volume would have a rotational relaxation time $\tau_D \sim 8.5$ ns, somewhat larger than the value that we observe.

We conclude that is is unlikely that the anisotropy decay

components are due to an equilibrium between two distinct conformations because a U-shaped conformer or a fully compacted molecule will not give an anisotropy decay time as short as the value we observed. So possibility ii above is unlikely.

The final possibility to consider is that the $tRNA_1^{Val}$ may have acquired significant internal flexibility, which would be expected if a weak spot of "hinge" were introduced into the molecule. It is known that Mg^{2+} interacts strongly with groups situated in the "knee" region of tRNA [see, e.g., Rigler & Wintermeyer (1983)] so that one might conjecture that Mg^{2+} could control a "hinge" in the tRNA by freeing or fixing residues in this region. Olson et al. (1976) have previously proposed the idea of such a hinge and our conception differs from theirs only in as much as we believe that Mg^{2+} rather than ionic strength per se is the principal controller of the hinge. Nilsson et al. (1982) modeled their small-angle X-ray scattering data by assuming that the tRNA arms could rotate about a hinge in the region of phosphates P_8 and P_{49}. However, the existence of such a joint could also facilitate local torsional or twisting motions within the molecule. These motions have been studied extensively in DNA (Allison & Schurr, 1979; Thomas et al., 1980; Thomas & Schurr, 1984), and we now discuss the likelihood of this behavior in tRNA giving rise to a substantial 6-ns anisotropy decay component.

Using the formalism of Allison & Schurr (1979), we can calculate both the relative amplitude and the time scale of any contribution that torsional deformations might make to the fluorescence anisotropy decay. In the Appendix, we carry out this calculation for a tRNA molecule consisting of two rodlike subunits interconnected by a Hookean torsion spring. We find that for a torsion spring constant $\alpha = 3.8 \times 10^{-12}$ dyn cm, which is the value characteristic of intact duplex DNA (Thomas & Schurr, 1980, 1983), the longest internal torsional mode will contribute $\sim$1.1% of the total anisotropy decay and that this mode (which is the slowest) has a relaxation time of $\sim$155 ps. Clearly, the magnitude of this contribution is too small and its relaxation time is much too short to give rise to the observed short decay time component.

We now ask the reverse question—what is the value for α that would contribute a substantial fraction of the anisotropy decay on a timescale of 6 ns? This calculation is also carried out in the Appendix, and we find that this requires $\alpha \sim 0.098 \times 10^{-12}$ dyn cm, which is $\sim$40 times weaker than that of an intact duplex DNA. With this value for α, the longest internal mode would account for $\sim$34% of the total anisotropy decay. We should expect that a localized hinge would be substantially weaker (more flexible) than native, linear DNA. Whether a 42-fold increase in flexibility is reasonable, we cannot say, but it is clear that we cannot dismiss the possibility of internal flexibility in $tRNA_1^{Val}$ contributing to the observed anisotropy decay.

Although the preceding analysis was based on segmental torsional motions, it was not intended to preclude bending motions. Such motions have been treated on numerous occasions (Harvey, 1979; Wegener, 1979, 1982; Harvey & Cheung, 1980; Harvey et al., 1983), but an accurate and convenient analytical result has not yet emerged, and simulations for the parameters of interest have not yet been carried out. Thus, quantitative predictions for elastic bending models to compare with our data are not yet at hand.

In summary, we find that when $tRNA_1^{Val}$ has all endogenous Mg^{2+} removed, it is not possible to titrate the Mg^{2+} directly back in and restore the original tRNA structure. Instead, titrating the $tRNA_1^{Val}$ with Mg^{2+} results in a multicomponent anisotropy decay that is not compatible with a simple change in the tertiary structure of the tRNA, nor is it compatible with a simple equilibrium between L-shaped and U-shaped conformers in solution. Rudimentary calculations show however that we cannot rule out the possibility of intramolecular torsional motions due perhaps to increased internal flexibility associated with the introduction of a hinge in the $tRNA_1^{Val}$ at increased Mg^{2+} concentrations. This behavior contrasts strongly with that of $tRNA^{Phe}$, where it seems that if Mg^{2+} is removed it can simply be titrated back in to restore the $tRNA^{Phe}$ to its native solution conformation.

In view of the present results, it is tempting to suggest that increased flexibility of the $tRNA_1^{Val}$ molecule compared with $tRNA^{Phe}$ may give rise to the different NMR spectral features mentioned at the outset. A more flexible molecule would give narrower spectral lines due to more complete orientational averaging. We could further speculate that the Mg^{2+}-dependent chemical shift in the 15–48 tertiary base pair may be associated with a torsion and/or flexion joint in that region, which could in turn give rise to a multicomponent FPA decay as outlined above.

Further work is in progress to establish more clearly the correlation between NMR and FPA results, but it is abundantly clear from the present work that removal of Mg^{2+} from $tRNA_1^{Val}$ causes irreversible changes to the tertiary structure of the molecule. Furthermore, $tRNA_1^{Val}$ and $tRNA^{Phe}$ display markedly different conformation behavior after the removal of Mg^{2+} despite the fact that prior to its removal the two tRNAs show essentially identical solution conformations.

Acknowledgments

Thanks are due to Kerrie Thomas for typing the manuscript.

Appendix

Contribution of Torsional Motion to the FPA Decay of EB/tRNA$_1^{Val}$. Allison & Schurr (1979) have developed a theory of the torsion dynamics of elastically deformable filaments based on a connected-rod model with arbitrary rod and contour lengths. Their eq 9 gives the correlation function for azimuthal rotation as

$$\langle \exp[ik[\theta(t) - \theta(0)]]\rangle_{T,R} = \frac{1}{N+1} \exp\left[\frac{-k^2 K_B T t}{(N+1)\gamma}\right] \sum_{m=1}^{N+1} \exp[-k^2 \sum_{l=2}^{N+1} d_l^2 Q_{ml}^2 [1 - \exp(t/\tau_l)]] \qquad k = 1, 2 \quad \text{(A1)}$$

where

$$\tau_l = \gamma/[4\alpha \sin^2 [(l-1)\pi/[2(N+1)]]] \quad \text{(A2)}$$

is the relaxation time of the lth normal (torsional) mode

$$d_l^2 = k_B T/[4\alpha \sin^2 [(l-1)\pi/[2(N+1)]]] \quad \text{(A3)}$$

is the amplitude of the lth normal mode, and

$$Q_{ml} = \left[\frac{2}{N+1}\right]^{1/2} \cos\left[\frac{(m-1/2)(l-1)\pi}{N+1}\right] \times (1 - \delta_{l,i}) + \delta_{l,i}\left[\frac{1}{N+1}\right]^{1/2} \qquad m = 1, \ldots, N+1 \quad \text{(A4)}$$

Here, $N+1$ is the number of rods, α is the torsion constant of the (Hookean) torsion springs that interconnect the rods, and γ is the rotational friction factor of the rods. k_B is the Boltzmann constant and T the absolute temperature.

At times $t \gg \tau_2$, the preexponential factor in eq A1 becomes (for $k = 2$)

$$B(\infty)_{k=2} = \frac{1}{N+1}\sum_{m=1}^{N+1} \exp[-4\sum_{l=2}^{N+1} d_l^2 Q_{ml}^2] \qquad (A5)$$

which is the decay amplitude *remaining* as we enter the timescale in which gross rotation of the macromolecule dominates the anisotropy relaxation.

Consider a tRNA molecule consisting of two rods each of length $h = 6.0$ nm and radius $a = 1.25$ nm (the radius of a double helix). We can calculate γ for the rods from the results of Perrin for the rotational friction factor

$$\gamma = 4\pi\eta a^2 h \qquad (A6)$$

where η is the solvent viscosity. At 20 °C in water, we calculate $\gamma = 118.1 \times 10^{-23}$ dyn cm.

For two rods, we have $N + 1 = 2$, $d_2^2 = k_B T/(2\alpha)$, $\tau_2 = \gamma/(2\alpha)$, and $Q_{1,2}^2 = Q_{2,2}^2 = 0.5$. Equation A5 then becomes

$$B(\infty)_{k=2} = \exp\left[\frac{-k_B T}{\alpha}\right]$$

and using $\alpha = 3.8 \times 10^{-12}$ dyn cm (which is the torsion constant measured for duplex DNA; Thomas et al., 1980), we get $B(\infty)_{k=2} = 0.989$ at 20 °C. Thus, for $\alpha = 3.8 \times 10^{-12}$ dyn cm, the longest internal mode ($l = 2$) contributes only $1.0 - 0.989 = 0.11$ of the total anisotropy decay. Moreover, this amplitude will decay on a time scale $\tau_2 = \gamma/(2\alpha) = 155$ ps. Clearly, here the amplitude is too small and the decay time is too short to be resolved in the present anisotropy data.

It is surely unreasonable to expect that, in a macromolecule as small as tRNA, a significant amplitude torsional motion (i.e., compared with uniform rotational motion) will occur at a site that has the same torsional rigidity as that of an intact linear DNA. More likely a torsional motion with a significant amplitude will be associated with a particular soft point or hinge in the tRNA. We can use the present data to estimate the torsional rigidity of such a hinge.

To be detected in the present experiments, the longest internal mode relaxation time would have to be $\tau_2 \sim 6$ ns. We can now calculate

$$\alpha = \gamma/(2\tau_2) \sim 0.0984 \times 10^{-12} \text{ dyn cm}$$

So, to contribute to the anisotropy relaxation on a timescale of ~6 ns, the torsion hinge would be ~3.8/0.0984 or ~40 times weaker than an intact linear duplex DNA. Now for this value of α we can go ahead and calculate the decay amplitude remaining at say $t = 30$ ns, which is the lifetime that we observe for the long-lived anisotropy component, i.e.

$$B(30)_{k=2} = \exp\left[\frac{-4k_B T(1 - e^{-30/6})}{4 \times 0.0984 \times 10^{-12}}\right] = 0.66$$

That is, with $\alpha \sim 0.098 \times 10^{-12}$ dyn cm, the longest internal (torsional) mode can account for at least 1.0–0.66 or ~34% of the total anisotropy decay that has occurred by 30 ns.

We see that internal torsional motions can account for a substantial fraction of the total anisotropy decay that occurs on the time scale of the rotational motion of the whole tRNA if we assume the presence of a hinge that is ~40 times weaker than intact linear DNA. We have not directly addressed the possibility of small-amplitude internal flexing motions contributing to the anisotropy decay; however, we anticipate that these motions would occur on a similar time scale and with an amplitude similar to the torsional motions. Thus, we conclude that internal torsional and/or flexing motions of the tRNA could account for the observed short-time anisotropy decay component.

Registry No. Mg, 7439-95-4.

References

Allison, S. A., & Schurr, J. M. (1979) *Chem. Phys. 41*, 35–39.

Belford, G. G., Belford, R. L., & Weber, G. (1983) *Proc. Natl. Acad. Sci. U.S.A. 69*, 1392–1393.

Bevington, P. R. (1969) *Data Reduction and Error Analysis for the Physical Sciences*, McGraw-Hill, New York.

Chuang, T. J., & Eisenthal, K. B. (1972) *J. Chem. Phys. 57*, 5094–5097.

Ehrenberg, M., & Rigler, R. (1972) *Chem. Phys. Lett. 14*, 539–544.

Ehrenberg, M., Rigler, R., & Wintermeyer, W. (1979) *Biochemistry 18*, 4588–4599.

Favre, A., & Thomas, G. (1981) *Annu. Rev. Biophys. Bioeng. 10*, 175–195.

Hare, D. (1983) Ph.D. Thesis, University of California at Riverside.

Harvey, S. C. (1979) *Biopolymers 18*, 1081–1104.

Harvey, S. C., & Cheung, H. C. (1980) *Biopolymers 19*, 913–930.

Harvey, S. C., Mellado, P., & Garcia de la Torre, J. (1983) *J. Chem. Phys. 78*, 2081–2090.

Nilsson, L., Rigler, R., & Laggner, P. (1982) *Proc. Natl. Acad. Sci. U.S.A. 79*, 5891–5895.

Olson, T., Fournier, M. J., Langley, K. H., & Ford, N. C. (1976) *J. Mol. Biol. 102*, 193–203.

Reid, B. R. (1977) in *Nucleic-Acid Protein Recognition* (Vogel, H. T., Ed.) pp 375–390, Academic Press, New York.

Reid, B. R., Ribeiro, N. S., McCollum, L., Abbate, J., & Hurd, R. E. (1977) *Biochemistry 16*, 2086–2094.

Rigler, R., & Wintermeyer, W. (1983) *Annu. Rev. Biophys. Bioeng. 12*, 475–505.

Tao, T. (1969) *Biopolymers 8*, 609–632.

Tao, T., Nelson, J. H., & Cantor, C. R. (1970) *Biochemistry 9*, 3514–3524.

Thomas, J. C., & Schurr, J. M. (1983) *Biochemistry 22*, 6194–6198.

Thomas, J. C., Allison, S. A., Appellof, C. J., & Schurr, J. M. (1980) *Biophys. Chem. 12*, 177–188.

Thomas, J. C., Schurr, J. M., & Hare, D. (1984) *Biochemistry* (preceding paper in this issue).

Wegener, W. (1979) *Biopolymers 19*, 1899–2008.

Wegener, W. (1982) *J. Chem. Phys. 76*, 6425–6430.

Yamakawa, H., & Fujii, M. (1973) *Macromolecules 6*, 407–415.